LETTER

doi:10.1038/nature14330

Icebergs not the trigger for North Atlantic cold events

Stephen Barker[1], James Chen[1]†, Xun Gong[1], Lukas Jonkers[1], Gregor Knorr[2] & David Thornalley[3,4]

Abrupt climate change is a ubiquitous feature of the Late Pleistocene epoch[1]. In particular, the sequence of Dansgaard–Oeschger events (repeated transitions between warm interstadial and cold stadial conditions), as recorded by ice cores in Greenland[2], are thought to be linked to changes in the mode of overturning circulation in the Atlantic Ocean[3]. Moreover, the observed correspondence between North Atlantic cold events and increased iceberg calving and dispersal from ice sheets surrounding the North Atlantic[4] has inspired many ocean and climate modelling studies that make use of freshwater forcing scenarios to simulate abrupt change across the North Atlantic region and beyond[5–7]. On the other hand, previous studies[4,8] identified an apparent lag between North Atlantic cooling events and the appearance of ice-rafted debris over the last glacial cycle, leading to the hypothesis that iceberg discharge may be a consequence of stadial conditions rather than the cause[4,9–11]. Here we further establish this relationship and demonstrate a systematic delay between pronounced surface cooling and the arrival of ice-rafted debris at a site southwest of Iceland over the past four glacial cycles, implying that in general icebergs arrived too late to have triggered cooling. Instead we suggest that—on the basis of our comparisons of ice-rafted debris and polar planktonic foraminifera—abrupt transitions to stadial conditions should be considered as a nonlinear response to more gradual cooling across the North Atlantic. Although the freshwater derived from melting icebergs may provide a positive feedback for enhancing and or prolonging stadial conditions[10,11], it does not trigger northern stadial events.

We investigated fluctuations in surface ocean temperature and the delivery of ice-rafted debris (IRD) to a site in the northeast Atlantic (Ocean Drilling Program (ODP) site 983; 60.4° N, 23.6° W, 1,984 m depth; Fig. 1) at high temporal resolution (177 years on average) over the past ~440 kyr (2,474 discrete samples). To this end we counted the relative proportion of the polar planktonic foraminifer, *Neogloboquadrina pachyderma*, within the total assemblage (%NPS; see Methods) and the number of lithogenic/terrigenous grains >150 μm per gram dry sediment (IRD per gram; see Methods). Today the location of ODP site 983 is under the influence of the warm surface Irminger Current (part of the modern subpolar gyre) as it turns northwards after splitting from the North Atlantic Current (NAC), which itself transports about 7.5 Sv (1 Sv = 10^6 m^3 s^{-1}) of warm (~8.5 °C) water over the Iceland–Scotland Ridge and into the Nordic Seas[12] (Fig. 1). This inflow is balanced in part by the outflow of cold fresh surface waters via the East Greenland Current but predominantly (~6 Sv) by overflows of cold dense bottom waters through the Denmark Strait and across the Iceland–Scotland Ridge that form as a result of strong wintertime cooling and convection within the Nordic Seas[12]. Together, these overflows represent the principal constituent precursors to North Atlantic Deep Water (NADW) and therefore represent an essential component of the modern Atlantic Meridional Overturning Circulation (AMOC)[12].

The present ingress of warm NAC waters into the Nordic Seas is reflected by the southwest–northeast orientation of the North Atlantic polar front (Fig. 1). During the Last Glacial Maximum (LGM; ~23,000–19,000 years ago, that is ~23–19 kyr ago) the polar front was positioned much further south and was more zonally orientated[13] (Fig. 1), suggesting a reduction in heat transport into the Nordic Seas by the NAC. Palaeoceanographic reconstructions[14] and a range of model experiments[15] suggest that this difference was reflected by a change in the geometry of the AMOC, with the northern locus of deep water formation shifted to the south of Iceland. An analogous (though not identical) change is thought to have accompanied the abrupt shifts associated with stadial/interstadial transitions[16,17]. As can be seen from the modern and LGM distributions of *N. pachyderma* (Fig. 1), its relative abundance at ODP site 983 is sensitive to latitudinal movements of the polar front. The site is also in the general path of drifting ice originating from Iceland, Greenland and Scandinavia[4,18,19] (Extended Data Fig. 1). The IRD we identify in ODP site 983 is predominantly quartz and volcanic material (Extended Data Fig. 2), with the latter presumably sourced from Iceland[4,20] or Eastern Greenland[20] and we note that volcanic material sourced from these regions is one of the earliest arrivals within the broader episodes of ice rafting across much of the North Atlantic[4,20] (Extended Data Fig. 1). This suggests that our site is ideally positioned to detect ice-rafting events in their earliest stages.

Our results reveal the intimate association between ice rafting and high-latitude temperature variability over the last four glacial cycles with unprecedented detail (Fig. 2). The resolution of our records permits us to investigate the precise phasing between these parameters for a large number of transitions. Accordingly, we developed an algorithm for objectively assessing the temporal offsets between abrupt cooling (warming) events and the arrival (disappearance) of IRD (Methods) and we found a clear difference between episodes of cooling and warming (Fig. 3). For the majority of events, cooling (that is, an abrupt increase in %NPS) occurs before the arrival of IRD, whereas there is much closer alignment between warming and the disappearance of IRD. This result is insensitive to the choice of thresholds used to detect the transitions (Extended Data Fig. 3) and for a reasonable range of threshold values we can state that the appearance of IRD lags behind cooling for at least 75% of detected events with at least 50% of cooling events occurring more than 200 years before the arrival of icebergs. We can therefore state that if the arrival of IRD to ODP site 983 heralds the delivery of rafted ice to the broader North Atlantic[4,20] then icebergs were not the trigger for North Atlantic cold events. Occasionally, an increase in IRD may occur without a corresponding increase in %NPS (Fig. 2). This tends to happen when conditions are already cold and may reflect saturation of the %NPS proxy. Cooling events may also occur

[1]School of Earth and Ocean Sciences, Cardiff University, Cardiff CF10 3AT, UK. [2]Alfred Wegener Institute Helmholtz Centre for Polar and Marine Research, Bussestrasse 24, D-27570 Bremerhaven, Germany. [3]Department of Geography, University College London, London WC1E 6BT, UK. [4]Woods Hole Oceanographic Institution, Woods Hole, Massachusetts 02543, USA. †Present address: School of Biological Sciences, University of Bristol, Bristol BS8 1TH, UK.

©2015 Macmillan Publishers Limited. All rights reserved

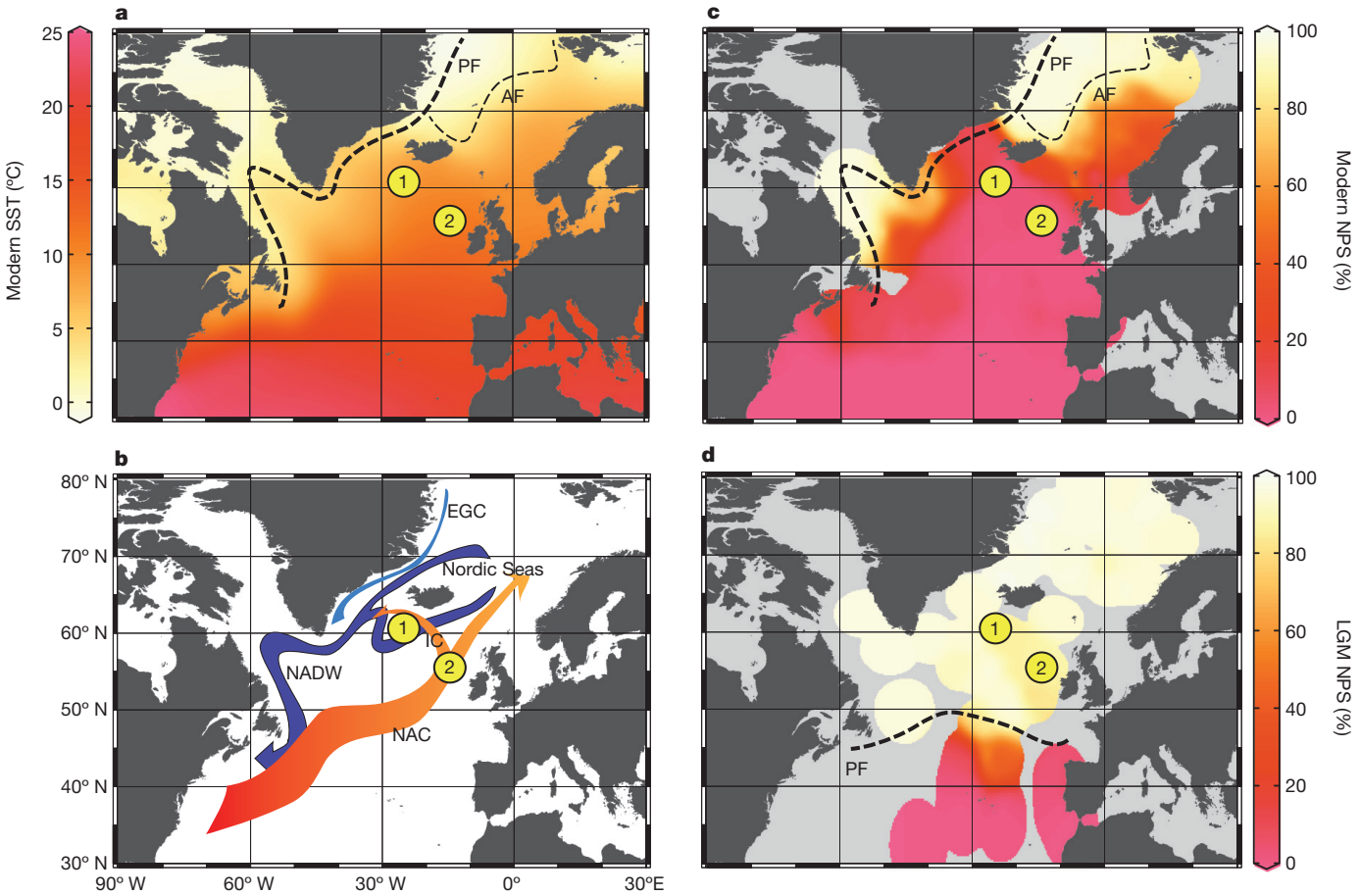

Figure 1 | Regional context of the study site. a, Modern sea surface temperature (SST)[29] shown on colour scale in degrees Celsius. PF, polar front; AF, Arctic front. **b**, Major ocean currents. NAC, North Atlantic Current; IC, Irminger Current; EGC, East Greenland Current; NADW, North Atlantic Deep Water. **c**, **d**, Modern and LGM distribution of %NPS (shown on colour scale)[13]. Also shown are the locations of ODP site 983 (point 1) and ODP site 980 (point 2). The figure was generated using Ocean Data View software (http://odv.awi.de/).

without a corresponding peak in IRD. Typically, this happens earlier in a glacial cycle and may reflect the smaller size of continental ice sheets at these times. Again, this suggests that icebergs are not necessary to initiate cold events.

Notably, the asynchrony we observe between temperature and IRD at ODP site 983 does not characterize the whole of the North Atlantic. When we apply our algorithm to equivalent records from ODP site 980 (~750 km to the southeast of our site; 55.5° N, 14.7° W, 2,180 m depth; Fig. 1)[21,22] we find that both cooling and warming transitions are aligned with the appearance and disappearance of IRD, respectively (Fig. 3). The surface records from ODP sites 983 and 980 can be aligned by tuning their respective benthic $\delta^{18}O$ records (Fig. 4). Although this approach lacks precision on a millennial-timescale it is clear that cold events at ODP site 983 last longer than those at ODP site 980 and typically start earlier. Furthermore, considering the general relations between temperature and IRD depicted in Fig. 3, the most parsimonious solution is the alignment of warming between the sites. This is in line with the current consensus that abrupt warming events may be considered as essentially synchronous across the wider North Atlantic region[23] and is consistent with modelling studies using both hosing (freshwater perturbation) and non-hosing scenarios[7,16,24]. It also implies that the IRD events observed at ODP sites 983 and 980 were approximately coeval and could therefore reflect more widespread ice rafting across the North Atlantic. The observation that cooling (implied by an abrupt increase in %NPS) at ODP site 983 may occur hundreds to thousands of years earlier than at ODP site 980 is at odds with model simulations using freshwater forcing to trigger cold events, which typically predict wholesale regional cooling within a few decades[5–7].

Instead, we suggest that the diachronous nature of cooling transitions recorded at ODP sites 983 and 980 can be explained by more gradual regional cooling and corresponding southward migration of the polar front (Fig. 4). The relative positions of ODP sites 983 and 980 means that transport of warm surface waters into the Nordic Seas could be maintained even if the polar front had migrated south of ODP site 983 (yet was still north of ODP site 980). With continued cooling the northward surface heat transport would decrease below the threshold necessary to sustain vigorous convection in the Nordic Seas (point B in Fig. 4c). At this point we suggest that the main locus of deep convection would shift to the south of Iceland as the AMOC switched from a warm to cold (stadial) mode[16]. This would coincide with a sharp increase in seasonal sea ice cover across the Nordic Seas and consequently much lower winter temperatures over Greenland as the climate entered a stadial state[25]. The abrupt transition to stadial conditions would result in rapid cooling across much of the North Atlantic[6,16], including ODP site 980 and south of the NAC (Fig. 4).

Studies suggest that the build-up of sub-surface heat in the high-latitude North Atlantic during stadials[17] may cause an increase in iceberg calving[9–11] (Methods). In combination with lower temperatures allowing wider dispersal of icebergs, this could explain the (approximately) simultaneous appearance of IRD across the wider North Atlantic at these times and suggests that the appearance of IRD at ODP site 983 is indicative of a transition to stadial conditions. This assertion is supported by the record of benthic foraminiferal $\delta^{13}C$

©2015 Macmillan Publishers Limited. All rights reserved

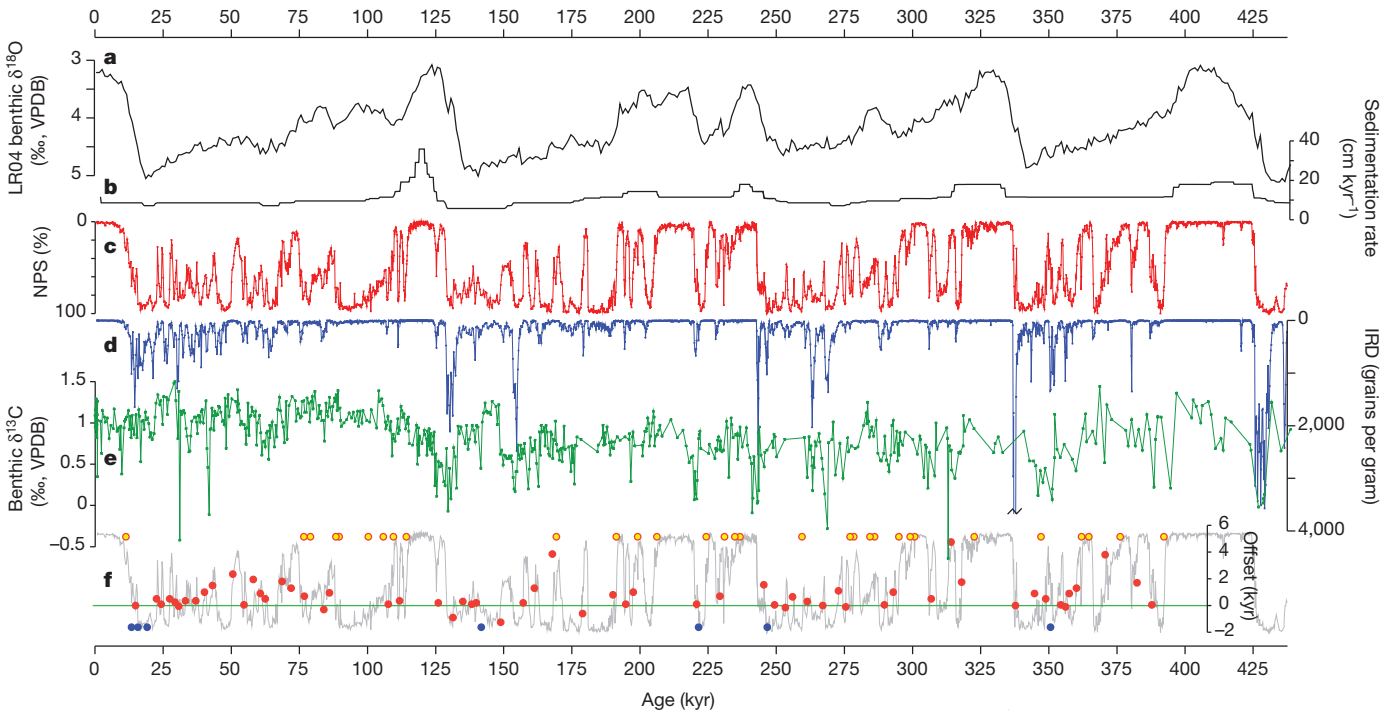

Figure 2 | Proxy records from ODP site 983. a, The LR04 benthic $\delta^{18}O$ stack[30]. **b**, Sedimentation rates in ODP site 983 according to the LR04 age model[30]. **c**, %NPS. **d**, IRD per gram. **e**, Benthic foraminiferal $\delta^{13}C$ (ref. 26). **f**, Red symbols are calculated offsets between cooling (increasing %NPS) and the arrival of IRD (a positive offset signifies that cooling occurs first). Yellow symbols are cooling events without corresponding IRD peaks and blue symbols are IRD events without registered cooling (see text for explanation). All records are plotted on the LR04 age model[30].

from ODP site 983 (ref. 26) (Fig. 2 and Extended Data Figs 4–7). Although the $\delta^{13}C$ record generally has lower temporal resolution than our records it is apparent that minima in benthic $\delta^{13}C$ tend to be shorter in duration than the cold events, as defined by %NPS, and more in line with the delivery of IRD[27]. Previous studies have interpreted low benthic $\delta^{13}C$ values at ODP site 983 to reflect increased sea ice cover over the Nordic Seas[26] or the enhanced influence of an underlying (southern-sourced) water mass with low $\delta^{13}C$ (ref. 27). Both of these conditions may be met when ocean circulation is in a stadial mode and thus the correspondence between IRD and benthic $\delta^{13}C$ implies that cooling at ODP site 983 occurs before the transition to stadial conditions.

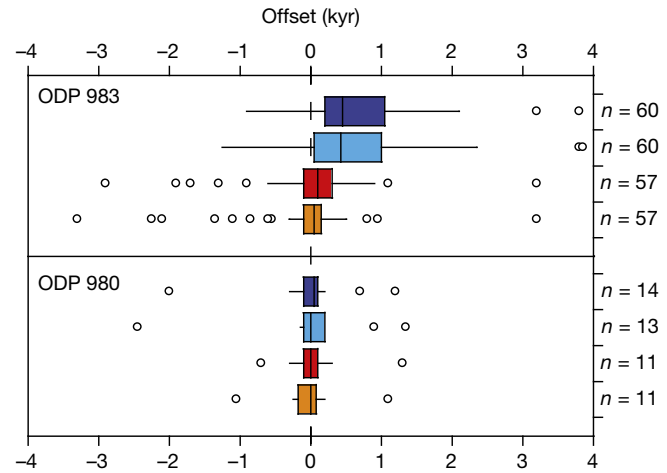

Figure 3 | Relative timing of temperature change versus ice rafting. Calculated offsets between temperature change (change in %NPS) and IRD at ODP site 983 (440–0 kyr ago) and ODP site 980 (440–360 kyr ago and 140–70 kyr ago)[21,22]. All analyses performed using the LR04 age model and identical threshold parameters (Methods). Boxes represent the interquartile range (IQR) dissected by the median value. Whiskers are 1.5 × IQR and extend to the last value included in this range. Positive values signify that temperature change is earlier. Blue boxes represent cooling versus arrival of IRD; red/orange boxes represent warming versus IRD decrease. Dark blue/red boxes represent the start of a transition; light blue/orange boxes reflect the midpoint. *n* = number of paired transitions detected.

Our observations have important chronologic implications because they suggest that a distinction should be made between stadial events *sensu stricto* (as recorded by Greenland ice cores) and North Atlantic cold events in their wider sense. Specifically, we suggest that sites to the northwest of the NAC may experience pronounced cooling (that is, a transition to Arctic/polar conditions) before the onset of Greenland stadial conditions, while those south of the NAC cool in phase with the transition to a stadial state. Indeed, a previous study from north of the NAC noted a systematic lag of 220 ± 100 years between abrupt cooling events at their site and the arrival of IRD during Marine Isotope Stage (MIS) 3 (ref. 8). On the other hand, we would expect sites throughout the North Atlantic region (both north and south of the NAC) to experience more gradual cooling before the transition to stadial conditions (as observed over Greenland[2,28]) and we note that Bond and Lotti[4] observed longer-term coolings before the arrival of IRD for several events during MIS 3. On the basis of these arguments we develop a strategy for refining the age model of ODP site 983 that can be used in future studies (see Methods and Extended Data Figs 4–8).

Our findings suggest that stadial transitions may occur as a nonlinear response to more gradual cooling, implying the existence of a threshold beyond which the transition to a stadial state becomes inevitable (Fig. 4). Indeed, the presence of such a threshold is apparent from the Greenland temperature record itself, with the duration of interstadials being a function of the rate of interstadial cooling[28] (Extended Data Fig. 9). Our results therefore support suggestions that abrupt climate transitions on millennial timescales are strongly dependent on internal feedbacks within the climate system (Methods). Increased iceberg calving and dispersal during stadials may provide a positive feedback on the AMOC, enhancing and/or prolonging stadial conditions through the addition of

©2015 Macmillan Publishers Limited. All rights reserved

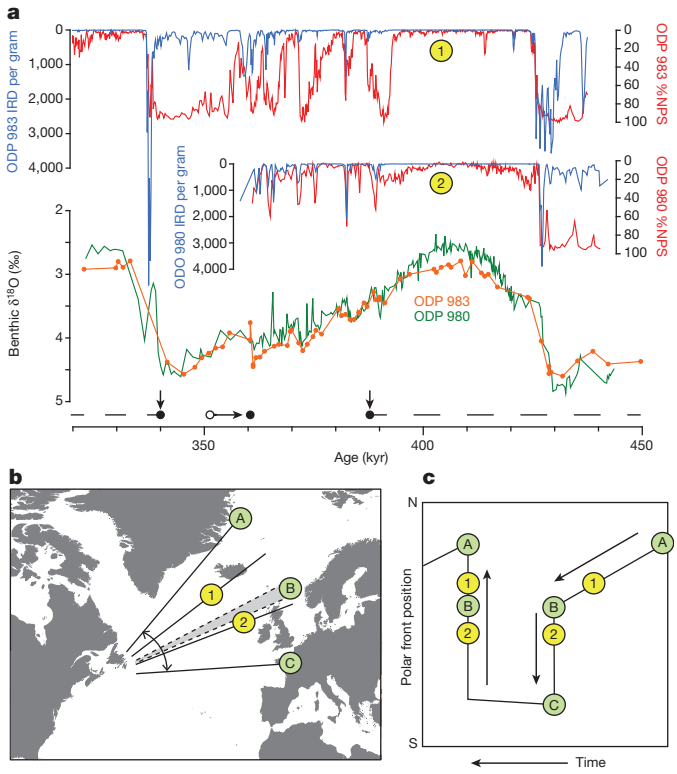

Figure 4 | Gradual cooling precedes the transition to stadial conditions. **a**, Records of %NPS and IRD per gram from ODP site 983 and 980 (ref. 21) reveal earlier cooling and longer cold intervals at the northern site (Methods). **b**, Cartoon showing approximate migration path of the polar front (1 and 2 are the positions of ODP sites 983 and 980). **c**, Schematic of the proposed time evolution of polar front movement. From point A, gradual cooling pushes the polar front southwards, crossing ODP site 983. On reaching threshold point B an abrupt southward migration of the polar front occurs with the transition to stadial conditions (point C). The return to warm conditions is essentially synchronous across the North Atlantic.

freshwater (with Heinrich events being the ultimate expression)[9–11,24]. However, these events should be viewed as a consequence of stadial conditions and not the driver.

Online Content Any additional Methods, Extended Data display items and Source Data, are available in the online version of the paper; references unique to these sections appear only in the online paper.

Received 16 September 2014; accepted 13 February 2015.

1. Jouzel, J. *et al.* Orbital and millennial Antarctic climate variability over the past 800,000 years. *Science* **317,** 793–796 (2007).
2. North Greenland Ice Core Project members. High-resolution record of Northern Hemisphere climate extending into the last interglacial period. *Nature* **431,** 147–151 (2004).
3. Broecker, W. S., Peteet, D. M. & Rind, D. Does the ocean-atmosphere system have more than one stable mode of operation? *Nature* **315,** 21–26 (1985).
4. Bond, G. C. & Lotti, R. Iceberg discharges into the North Atlantic on millennial time scales during the last glaciation. *Science* **267,** 1005–1010 (1995).
5. Rahmstorf, S. Rapid climate transitions in a coupled ocean-atmosphere model. *Nature* **372,** 82–85 (1994).
6. Vellinga, M. & Wood, R. A. Global climatic impacts of a collapse of the Atlantic thermohaline circulation. *Clim. Change* **54,** 251–267 (2002).
7. Kageyama, M. *et al.* Climatic impacts of fresh water hosing under Last Glacial Maximum conditions: a multi-model study. *Clim. Past* **9,** 935–953 (2013).
8. van Kreveld, S. *et al.* Potential links between surging ice sheets, circulation changes, and the Dansgaard-Oeschger cycles in the Irminger Sea, 60–18 kyr. *Paleoceanography* **15,** 425–442 (2000).
9. Shaffer, G., Olsen, S. M. & Bjerrum, C. J. Ocean subsurface warming as a mechanism for coupling Dansgaard-Oeschger climate cycles and ice-rafting events. *Geophys. Res. Lett.* **31,** L24202 (2004).
10. Clark, P. U., Hostetler, S. W., Pisias, N. G., Schmittner, A. & Meissner, K. J. Mechanisms for an 7-kyr climate and sea-level oscillation during Marine Isotope Stage 3. *Ocean Circulation: Mechanisms and Impacts—Past and Future Changes of Meridional Overturning* (eds Schmittner, A. Chiang, J. C. H. & Hemming, S. R.) 209–246 (AGU, 2007).
11. Alvarez-Solas, J., Robinson, A., Montoya, M. & Ritz, C. Iceberg discharges of the last glacial period driven by oceanic circulation changes. *Proc. Natl Acad. Sci. USA* **110,** 16350–16354 (2013).
12. Dickson, R. R. & Brown, J. The production of North Atlantic DeepWater—sources, rates, and pathways. *J. Geophys. Res. Oceans* **99,** 12319–12341 (1994).
13. MARGO Project members. Constraints on the magnitude and patterns of ocean cooling at the Last Glacial Maximum. *Nature Geosci.* **2,** 127–132 (2009).
14. Sarnthein, M. *et al.* Changes in East Atlantic deep-water circulation over the last 30,000 years: eight time slice reconstructions. *Paleoceanography* **9,** 209–267 (1994).
15. Weber, S. L. *et al.* The modern and glacial overturning circulation in the Atlantic Ocean in PMIP coupled model simulations. *Clim. Past* **3,** 51–64 (2007).
16. Ganopolski, A. & Rahmstorf, S. Rapid changes of glacial climate simulated in a coupled climate model. *Nature* **409,** 153–158 (2001).
17. Ezat, M. M., Rasmussen, T. L. & Groeneveld, J. Persistent intermediate water warming during cold stadials in the southeastern Nordic seas during the past 65 k.y. *Geology* **42,** 663–666 (2014).
18. Death, R., Siegert, M. J., Bigg, G. R. & Wadley, M. R. Modelling iceberg trajectories, sedimentation rates and meltwater input to the ocean from the Eurasian Ice Sheet at the Last Glacial Maximum. *Palaeogeogr. Palaeoclimatol. Palaeoecol.* **236,** 135–150 (2006).
19. Watkins, S., Maher, B. & Bigg, G. Ocean circulation at the Last Glacial Maximum: a combined modeling and magnetic proxy-based study. *Paleoceanography* **22,** PA2204 (2007).
20. Jullien, E. *et al.* Contrasting conditions preceding MIS3 and MIS2 Heinrich events. *Global Planet. Change* **54,** 225–238 (2006).
21. Oppo, D. W., McManus, J. F. & Cullen, J. L. Abrupt climate events 500,000 to 340,000 years ago: evidence from subpolar north Atlantic sediments. *Science* **279,** 1335–1338 (1998).
22. Oppo, D. W., McManus, J. F. & Cullen, J. L. Evolution and demise of the Last Interglacial warmth in the subpolar North Atlantic. *Quat. Sci. Rev.* **25,** 3268–3277 (2006).
23. Austin, W. E. & Hibbert, F. D. Tracing time in the ocean: a brief review of chronological constraints (60–8 kyr) on North Atlantic marine event-based stratigraphies. *Quat. Sci. Rev.* **36,** 28–37 (2012).
24. Knorr, G. & Lohmann, G. Rapid transitions in the Atlantic thermohaline circulation triggered by global warming and meltwater during the last deglaciation. *Geochem. Geophys. Geosyst.* **8,** Q12006 (2007).
25. Li, C., Battisti, D. S. & Bitz, C. M. Can North Atlantic sea ice anomalies account for Dansgaard-Oeschger climate signals? *J. Clim.* **23,** 5457–5475 (2010).
26. Raymo, M. E. *et al.* Stability of North Atlantic water masses in face of pronounced climate variability during the Pleistocene. *Paleoceanography* **19,** PA2008 (2004).
27. Kleiven, H. F., Hall, I. R., McCave, I. N., Knorr, G. & Jansen, E. Coupled deep-water flow and climate variability in the middle Pleistocene North Atlantic. *Geology* **39,** 343–346 (2011).
28. Schulz, M. The tempo of climate change during Dansgaard-Oeschger interstadials and its potential to affect the manifestation of the 1470-year climate cycle. *Geophys. Res. Lett.* **29,** http://dx.doi.org/10.1029/2001GL013277(2002).
29. Locarnini, R. A. *et al.* in *NOAA Atlas NESDIS 68* (ed. Levitus, S.) 184 (US Government Printing Office, 2010).
30. Lisiecki, L. E. & Raymo, M. E. A. Pliocene-Pleistocene stack of 57 globally distributed benthic $\delta^{18}O$ records. *Paleoceanography* **20,** http://dx.doi.org/10.1029/2004PA001071 (2005).

Supplementary Information is available in the online version of the paper.

Acknowledgements We thank S. Edwards, L. Owen, F. Piggott, L. Skyrme and M. Theobald for assistance in the laboratory and J. McManus for discussions. This study was supported by a Philip Leverhulme Prize to S.B., the Comer Science and Education Foundation (GCCF3) and the UK Natural Environment Research Council (NERC) grants NE/L006405/1 and NE/J008133/1. Additional funding by 'Helmholtz Climate Initiative REKLIM' (Regional Climate Change), a joint research project of the Helmholtz Association of German research centres (HGF), is gratefully acknowledged (G.K.). L.J. was funded by the climate change consortium of Wales (http://www.C3Wales.org). This research used samples provided by the Integrated Ocean Drilling Program (IODP). We thank W. Hale for assistance in sampling and curation. All data and age models presented here are available in the Extended Data.

Author Contributions S.B. designed research and analysed datasets. J.C. processed samples and performed faunal counts with assistance from those mentioned in the Acknowledgements. X.G. performed ice core data analysis. S.B., L.J., X.G., G.K. and D.T. contributed to writing the paper.

Author Information Reprints and permissions information is available at www.nature.com/reprints. The authors declare no competing financial interests. Readers are welcome to comment on the online version of the paper. Correspondence and requests for materials should be addressed to S.B. (barkers3@cf.ac.uk).

©2015 Macmillan Publishers Limited. All rights reserved

METHODS

Sample preparation and faunal counts. Sediment samples were spun overnight and washed with deionized water through a 63-μm sieve before being dried at 40 °C. IRD and faunal counts were made on the >150 μm fraction after splitting to yield approximately 300 entities. Only left-coiling specimens of *N. pachyderma* were counted and those with morphological resemblance to *Neogloboquadrina incompta* were not counted. The uncertainty due to aberrant coiling in *N. pachyderma* is therefore <3% (ref. 31). The percentage of *N. pachyderma* in the North Atlantic can be used as a sensitive tracer for the locations of oceanic fronts in this region (Fig. 1). According to Pflaumann *et al.*[32] the Arctic front is documented by the transition from ~90%–94% NPS, while values of ~98% NPS track the polar front. IRD was considered to be the total number of lithogenic/terrigenous grains counted. The majority of grains fall into two categories: quartz and volcanics, with volcanics comprising ~36% of the total IRD on average (Extended Data Fig. 2).

Temporal offsets between temperature change and IRD input. *Code availability.* Temporal offsets were determined using an algorithm developed in Matlab (the script is available as a Matlab file in the Supplementary Information).

All datasets were input in the time domain (equivalent results were obtained using the depth domain) using the LR04 timescale[30] (a revised age model was also used for comparison, Extended Data Fig. 8) and evenly resampled at 0.1 kyr intervals (similar to the physical sampling rate during interglacial periods, when sedimentation rates are greatest). Records were then smoothed using a rectangular filter (running mean) of 0.5 kyr (similar to the lowest sampling rate during full glacial periods) implemented by *filtfilt* in Matlab (that is, run forward and reverse) and differentiated with respect to time (via the difference quotient). Abrupt transitions in %NPS or IRD per gram then identified by their respective derivatives exceeding a threshold. When looking for cooling events, the algorithm is primed by the completion of a warming event according to % NPS (completion of an IRD event serves as an alternative primer). It then searches for the next time %NPS and/or IRD per gram increases at a rate greater than a given threshold (specific to each parameter). The algorithm is reset when warming next occurs. Warming offsets (decrease in %NPS and IRD per gram) are quantified in an analogous way with a threshold value equal to −1 times that used for the cooling offsets. The algorithm identifies the onset of a transition as the time when the threshold is first exceeded and the mid-point of the transition as the mid-point of all consecutive points exceeding the threshold. We calculate offsets for both the start and mid-point of transitions since the mid-point is less sensitive to the specific threshold values employed. However, we find a similar result using either approach (Fig. 3). The algorithm rejects offsets outside of a given range, in this case ±6 kyr.

The detection of individual events depends on a trade-off between the length of smoothing window applied (which is common to all records) and the derivative threshold values employed (which are specific to each record). To determine the optimal set of threshold values we performed a sensitivity analysis (Extended Data Fig. 3). If a threshold is too sensitive or too insensitive it is less likely that a true pair of transitions will be identified, leading to an erroneous calculated offset. This effect is apparent from offsets calculated for warming events. It can be seen that the interquartile range (IQR) for warming offsets is larger when the thresholds are at the lower or upper limits of our sensitivity analysis. An equivalent result is obtained when IRD is used as a primer. We suggest that the most appropriate threshold pairs should result in smaller values of the IQR for warming transitions (implying greater consistency between individual events). From the results shown in Extended Data Fig. 3 we use this principle to delineate a region of optimal threshold values. We employ the lower left set of values within this range in Fig. 3 because it results in the highest number of paired transitions. It is also the most conservative in terms of the calculated offsets (other pairings result in more positive offsets).

Alignment of records from ODP site 983 and ODP site 980. See Fig. 4. The cores were aligned by modifying the LR04 age model[30] to improve alignment of their benthic $\delta^{18}O$ records. In Fig. 4, records from ODP site 980 are on LR04 throughout. Those from ODP site 983 are on LR04 for the dashed intervals. Between these anchor points the age model for ODP site 983 has been shifted as indicated by the horizontal black arrow.

Stadial transitions as a nonlinear response to gradual cooling. Since Bond and Lotti's[4] observation that most Greenland stadial events (not just those related to Heinrich events) were associated with increased iceberg calving and dispersal across the North Atlantic region, a great number of ocean and climate modelling studies have employed freshwater forcing scenarios to simulate abrupt change across the North Atlantic region and beyond[5–7,33,34]. Clearly the influence of freshwater on the efficacy of NADW formation has important consequences for the AMOC, and mechanisms that invoke (quasi-) periodic fluctuations in iceberg calving and freshwater input provide an appealing solution to the question of why Greenland stadials (and North Atlantic Heinrich events) occur with such regularity[35–37]. However, the observations that cooling—both abrupt (this study and ref. 8) and gradual (ref. 4)—across the North Atlantic actually precedes the transition to stadial conditions (and therefore the release of icebergs) suggests that an alternative to freshwater forcing from icebergs should be considered as the trigger for inducing stadial transitions. Accordingly, several previous studies have invoked abrupt transitions in ocean circulation without calling on iceberg discharge as a primary forcing agent[10,38–44].

On the basis of our observations we invoke gradual cooling across the North Atlantic region as the ultimate trigger for the transition to stadial conditions. Thus we consider stadial transitions as an abrupt, nonlinear response to more gradual forcing. The precise cause(s) of cooling may be manifold and may vary depending on the background state. For example, longer-term cooling may be the result of changes in insolation, greenhouse gas forcing or ice sheet configuration[44]. On shorter timescales cooling could be induced by a gradual weakening of the AMOC either in response to a gradual freshening of the surface North Atlantic[38] or following a transient AMOC overshoot at the onset of interstadial conditions[24,33]. Alternatively, the build-up of circum-North Atlantic ice shelves could lead eventually to runaway cooling and the development of stadial conditions[43]. Once in a stadial state, the build-up of subsurface heat may lead to the destruction of ice shelves and ultimately the partial collapse of land-based ice sheets (with Heinrich events being the ultimate expression of such a mechanism)[4,9–11,43,45,46]. The freshwater provided as a consequence of such a collapse may be expected to enhance and /or prolong stadial conditions[10,24] and thus should be considered as a positive feedback rather than the initial trigger for stadial transitions.

Revised age model development. The site of ODP site 983 is positioned on the rapidly accumulating Gardar Drift and sediment accumulation is sensitive to changes in the dense overflows crossing the Iceland–Scotland Ridge[26,27], which themselves are thought to vary in concert with high-latitude climate[17,27]. At orbital timescales this can be seen through elevated sedimentation rates during interglacials (as implied by the LR04 age model[30]; Fig. 2), when the overflows are thought to be more vigorous[26,27], but this also implies that sedimentation rates are elevated during millennial-scale warm events that are not accounted for by the LR04 age model. Given the potentially large and frequent changes in sedimentation rate at ODP site 983 we require a more detailed tuning strategy for refining the age assignment of abrupt events within our records. A typical approach in the development of such an age model is to align abrupt changes in our records with those in a reference stratigraphy[23] such as GL_T_syn (a synthetic prediction of Greenland temperature)[47,48].

In line with previous studies[23,47] we assume that abrupt warming events in our record (which also align with the disappearance of IRD) are synchronous with warming across the wider North Atlantic region and align these with warming transitions in GL_T_syn[48] (Extended Data Figs 4–7). As mentioned, sedimentation at ODP site 983 is sensitive to the overflows crossing the Iceland–Scotland ridge[26,27], with elevated accumulation rates during warm intervals reflecting enhanced advection of fine (<63 μm) material to the site of ODP site 983 driven by faster currents crossing the Iceland–Faeroe ridge[26]. The coarse (>63 μm) fraction of ODP site 983 therefore reflects both the delivery of IRD (which increases during stadials) and the input of fine fraction (which decreases during stadials). We therefore align increases in the coarse fraction with cooling transitions in GL_T_syn. We tune our records to GL_T_syn on the EDC3 age model[49] and note that the implied changes in sedimentation rate are in line with expectations (higher during warmer intervals). We also convert the EDC3 ages to an alternative ice core age model (AICC2012[50,51]) and an absolute age model (GICC05/NALPS/China) based on previous studies[48,52–55] (see the source data associated with Extended Data Fig. 4).

Given the potential influence of the sedimentation rate changes implied by our new age model on the calculated offsets, we ran the algorithm on the data sets using the new age model (Extended Data Fig. 8). We note that the distribution of offsets is very similar for the two age models (LR04 versus our EDC3) although the median cooling offset (mid-transition) for the revised age model is slightly smaller at 350 years compared with 425 years when using LR04. This can be explained as a result of higher implied sedimentation rates (fewer years per sampled interval) during interstadial periods that extend beyond cooling (according to %NPS) until the arrival of IRD.

31. Darling, K. F., Kucera, M., Kroon, D. & Wade, C. M. A resolution for the coiling direction paradox in *Neogloboquadrina pachyderma*. *Paleoceanography* **21,** PA2011 (2006).

©2015 Macmillan Publishers Limited. All rights reserved

32. Pflaumann, U., Duprat, J., Pujol, C. & Labeyrie, L. D. SIMMAX: a modern analog technique to deduce Atlantic sea surface temperatures from planktonic foraminifera in deep-sea sediments. *Paleoceanography* **11,** 15–35 (1996).
33. Liu, Z. *et al.* Transient simulation of last deglaciation with a new mechanism for Bolling-Allerod warming. *Science* **325,** 310–314 (2009).
34. Menviel, L., Timmermann, A., Friedrich, T. & England, M. Hindcasting the continuum of Dansgaard–Oeschger variability: mechanisms, patterns and timing. *Clim. Past* **10,** 63–77 (2014).
35. MacAyeal, D. R. Binge/purge oscillations of the Laurentide ice sheet as a cause of the North Atlantic Heinrich events. *Paleoceanography* **8,** 775–784 (1993).
36. Alley, R. B., Anandakrishnan, S. & Jung, P. Stochastic resonance in the North Atlantic. *Paleoceanography* **16,** 190–198 (2001).
37. Braun, H. *et al.* Possible solar origin of the 1,470-year glacial climate cycle demonstrated in a coupled model. *Nature* **438,** 208–211 (2005).
38. Broecker, W. S., Bond, G. & Klas, M. A salt oscillator in the glacial Atlantic? 1. The concept. *Paleoceanography* **5,** 469–477 (1990).
39. Winton, M. & Sarachik, E. S. Thermohaline oscillations induced by strong steady salinity forcing of ocean general-circulation models. *J. Phys. Oceanogr.* **23,** 1389–1410 (1993).
40. Winton, M. The effect of cold climate upon North Atlantic Deep Water formation in a simple ocean-atmosphere model. *J. Clim.* **10,** 37–51 (1997).
41. Schulz, M., Paul, A. & Timmermann, A. Relaxation oscillators in concert: a framework for climate change at millennial timescales during the late Pleistocene. *Geophys. Res. Lett.* **29,** http://dx.doi.org/10.1029/2002GL016144 (2002).
42. Dokken, T. M., Nisancioglu, K. H., Li, C., Battisti, D. S. & Kissel, C. Dansgaard-Oeschger cycles: interactions between ocean and sea ice intrinsic to the Nordic seas. *Paleoceanography* **28,** 491–502 (2013).
43. Petersen, S., Schrag, D. & Clark, P. U. A new mechanism for Dansgaard-Oeschger cycles. *Paleoceanography* **28,** 24–30 (2013).
44. Zhang, X., Lohmann, G., Knorr, G. & Purcell, C. Abrupt glacial climate shifts controlled by ice sheet changes. *Nature* **512,** 290–294 (2014).
45. Alvarez-Solas, J. *et al.* Links between ocean temperature and iceberg discharge during Heinrich events. *Nature Geosci.* **3,** 122–126 (2010).
46. Marcott, S. A. *et al.* Ice-shelf collapse from subsurface warming as a trigger for Heinrich events. *Proc. Natl Acad. Sci. USA* **108,** 13415–13419 (2011).
47. Hodell, D. *et al.* Response of Iberian Margin sediments to orbital and suborbital forcing over the past 420 ka. *Paleoceanography* **28,** 185–199 (2013).
48. Barker, S. *et al.* 800,000 years of abrupt climate variability. *Science* **334,** 347–351 (2011).
49. Parrenin, F. *et al.* The EDC3 chronology for the EPICA dome C ice core. *Clim. Past* **3,** 485–497 (2007).
50. Bazin, L. *et al.* An optimized multi-proxy, multi-site Antarctic ice and gas orbital chronology (AICC2012): 120-800 ka. *Clim. Past* **9,** 1715–1731 (2013).
51. Veres, D. *et al.* The Antarctic ice core chronology (AICC2012): an optimized multi-parameter and multi-site dating approach for the last 120 thousand years. *Clim. Past* **9,.** 1733–1748 (2013).
52. Barker, S. & Diz, P. Timing of the descent into the last ice age determined by the bipolar seesaw. *Paleoceanography*, **29,** http://dx.doi.org/10.1002/2014PA002623 (2014).
53. Andersen, K. K. *et al.* A 60 000 year Greenland stratigraphic ice core chronology. *Clim. Past Discuss.* **3,** 1235– **1260,**(2007).
54. Boch, R. *et al.* NALPS: a precisely dated European climate record 120-60 ka. *Clim. Past* **7,** 1247–1259 (2011).
55. Cheng, H. *et al.* Ice age terminations. *Science* **326,** 248–252 (2009).
56. Ruddiman, W. F. Late Quaternary deposition of ice-rafted sand in the subpolar North Atlantic (lat 40 to 65 N). *Geol. Soc. Am. Bull.* **88,** 1813–1827 (1977).
57. Elliot, M. *et al.* Millennial-scale iceberg discharges in the Irminger Basin during the last glacial period: relationship with the Heinrich events and environmental settings. *Paleoceanography* **13,** 433–446 (1998).
58. Revel, M., Cremer, M., Grousset, F. E. & Labeyrie, L. Grain-size and Sr-Nd isotopes as tracer of paleo-bottom current strength, Northeast Atlantic Ocean. *Mar. Geol.* **131,** 233–249 (1996).
59. Moros, M. *et al.* Quartz content and the quartz-to-plagioclase ratio determined by X-ray diffraction: a proxy for ice rafting in the northern North Atlantic? Earth Planet. *Sci. Lett.* **218,** 389–401 (2004).
60. Prins, M. A. *et al.* Ocean circulation and iceberg discharge in the glacial North Atlantic: inferences from unmixing of sediment size distributions. *Geology* **30,** 555–558 (2002).
61. Jonkers, L. *et al.* A reconstruction of sea surface warming in the northern North Atlantic during MIS 3 ice-rafting events. *Quat. Sci. Rev.* **29,** 1791–1800 (2010).
62. Scourse, J. D., Hall, I. R., McCave, I. N., Young, J. R. & Sugdon, C. The origin of Heinrich layers: evidence from H2 for European precursor events. *Earth Planet. Sci. Lett.* **182,** 187–195 (2000).
63. Grousset, F. E., Pujol, C., Labeyrie, L., Auffret, G. & Boelaert, A. Were the North Atlantic Heinrich events triggered by the behavior of the European ice sheets? *Geology* **28,** 123–126 (2000).
64. Grousset, F. E. *et al.* Zooming in on Heinrich layers. *Paleoceanography* **16,** 240–259 (2001).

©2015 **Macmillan Publishers Limited. All rights reserved**

a

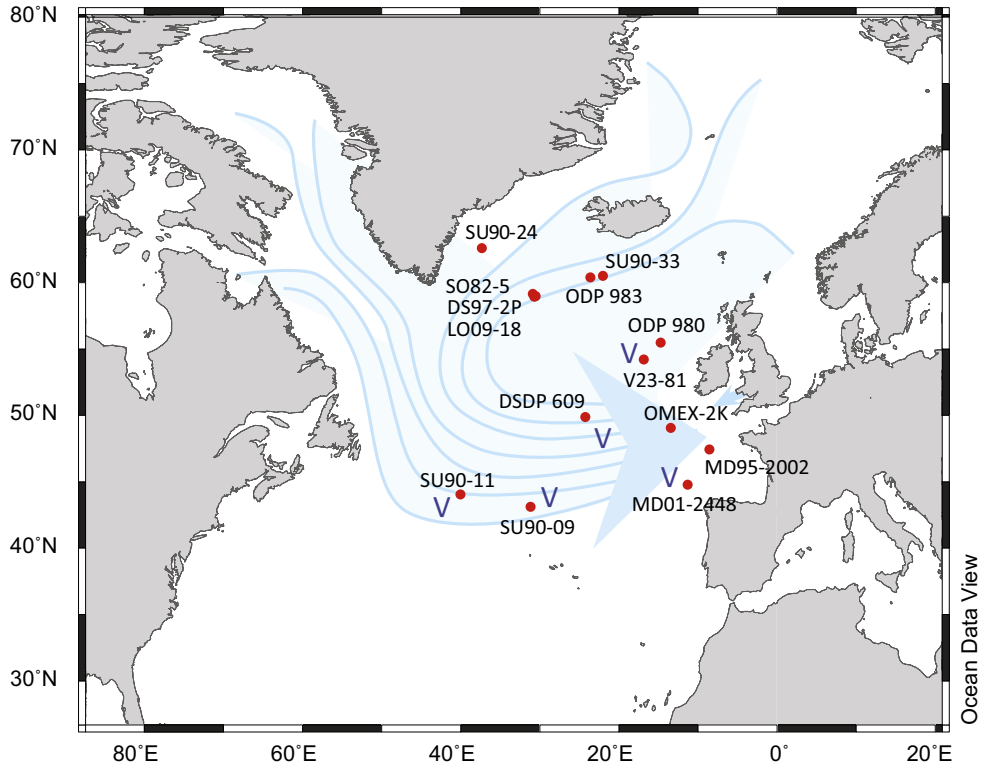

b

Core ID	Lat	Long	Provenance				Reference
			Iceland (volcanics)	European	Greenland	Hudson Strait	
SU90-24	62.6	-37.3	YES	MAYBE	MAYBE	NO	Elliot et al., 1998 (57)
SU90-33	60.5	-22.0	YES	YES	MAYBE	NO	Revel et al., 1996 (58)
ODP 983	60.4	-23.6	YES	MAYBE	MAYBE	NO	This study
SO82-5	59.2	-30.9	YES	YES	YES	NO	van Kreveld et al., 2000 (8); Moros et al., 2004 (59)
DS97-2P	59.0	-30.5	YES	-	YES	-	Prins et al., 2002 (60); Jonkers et al., 2010 (61)
LO09-18	59.0	-30.7	YES	YES	YES	NO	Moros et al., 2004 (59); Jonkers et al., 2010 (61)
ODP 980	55.5	-14.7	-	-	-	-	Oppo et al., 1998; 2006 (21, 22)
V23-81	54.3	-16.8	EARLY	MAYBE	MAYBE	LATE	Bond and Lotti, 1995 (4)
DSDP609	49.9	-24.2	EARLY	MAYBE	MAYBE	LATE	Bond and Lotti, 1995 (4)
OMEX-2K	49.1	-13.4	-	EARLY	-	YES	Scourse et al., 2000 (62)
MD95-2002	47.5	-8.5	YES	EARLY and LATE	-	YES	Grouset et al., 2000 (63)
MD01-2448	44.8	-11.3	EARLY	YES	MAYBE	YES	Julien et al., 2006 (20)
SU90-11	44.1	-40.0	EARLY	YES	MAYBE	YES	Julien et al., 2006 (20)
SU90-09	43.1	-31.1	EARLY	YES	-	LATE	Grouset et al., 2001 (64)

Extended Data Figure 1 | North Atlantic iceberg trajectories. a, Map showing locations of core sites relevant to this study with simplified iceberg trajectories, after ref. 56. Sites where volcanics are reported to appear early within broader pulses of IRD are marked with a 'V'. **b**, Core details and summary of IRD sources for each site[4,20–22,57–64]. In line with our observation of early cooling with respect to ice rafting at ODP site 983, early cooling has also been reported at sites SO82-5[8], DS97-2P[61] and LO09-18[61] within the Irminger Sea.

©2015 Macmillan Publishers Limited. All rights reserved

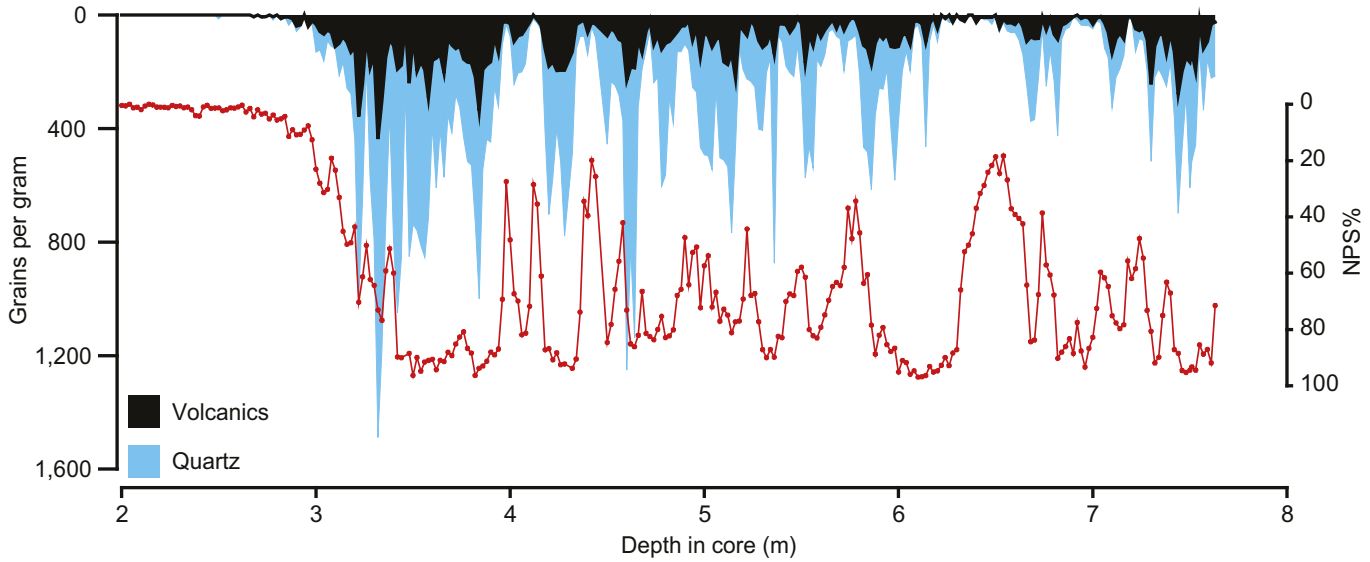

Extended Data Figure 2 | IRD composition at ODP site 983. Volcanics comprise ~36% of the total IRD on average.

©2015 Macmillan Publishers Limited. All rights reserved

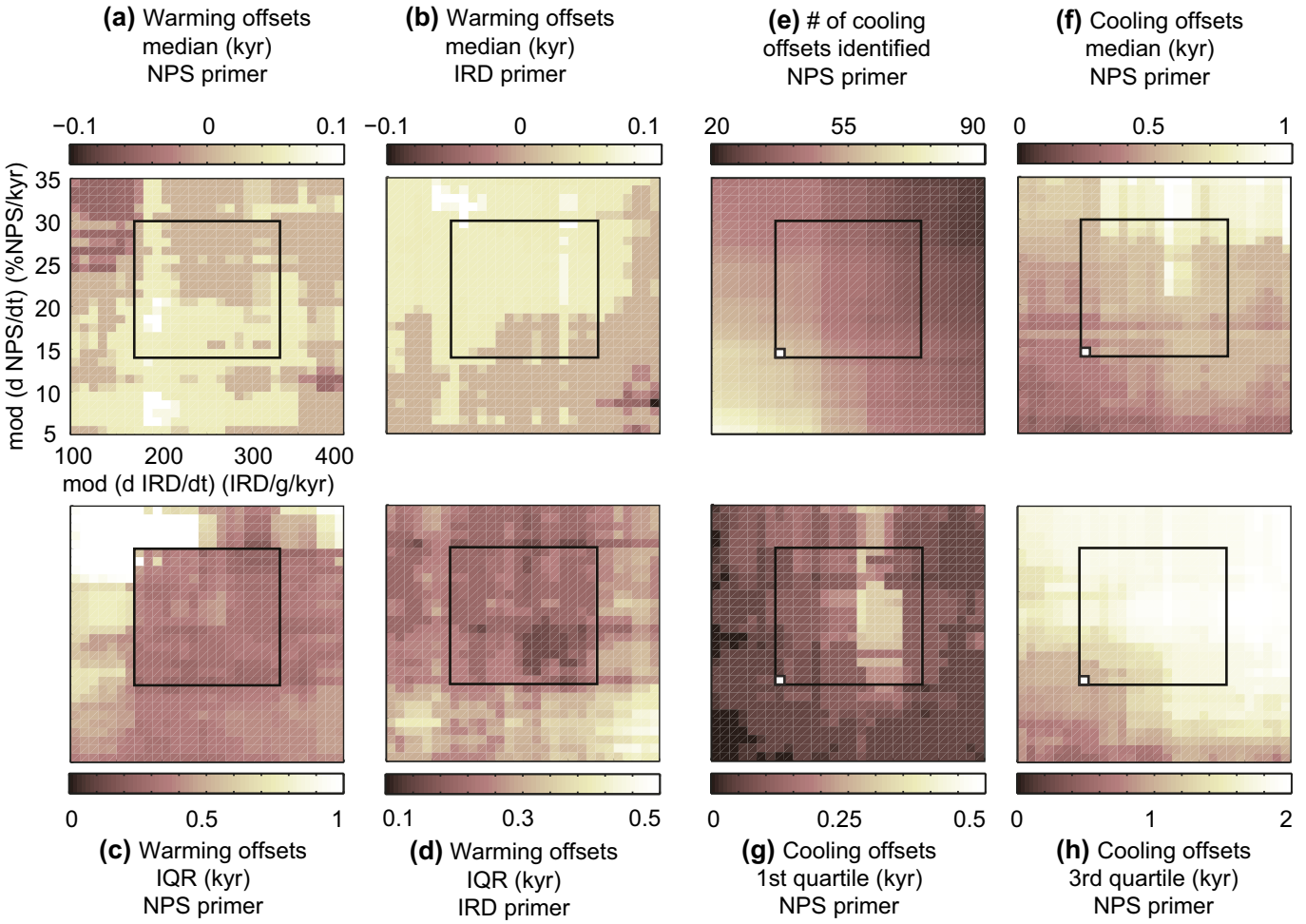

Extended Data Figure 3 | Threshold sensitivity analysis for the calculation of offsets between temperature and IRD. a, **b**, Warming offsets are small (typically 0–50 yr) for a wide range of thresholds using either %NPS or IRD per gram as the primer (Methods) but the IQR (**c**, **d**) is larger for more or less sensitive thresholds. We define an optimal set of threshold values as those producing lower values for the IQR (delineated by the black square). **e**, Decreasing the threshold sensitivity (higher rates of change required to detect a transition) results in fewer paired transitions. Small white square is the threshold set that gives the highest number of paired transitions within optimal region and is used in Fig. 3 (dNPS/dt = ±14, dIRD/dt = ±170). **f**, **h**, Cooling offsets are all positive for the first, median and third quartiles.

©2015 Macmillan Publishers Limited. All rights reserved

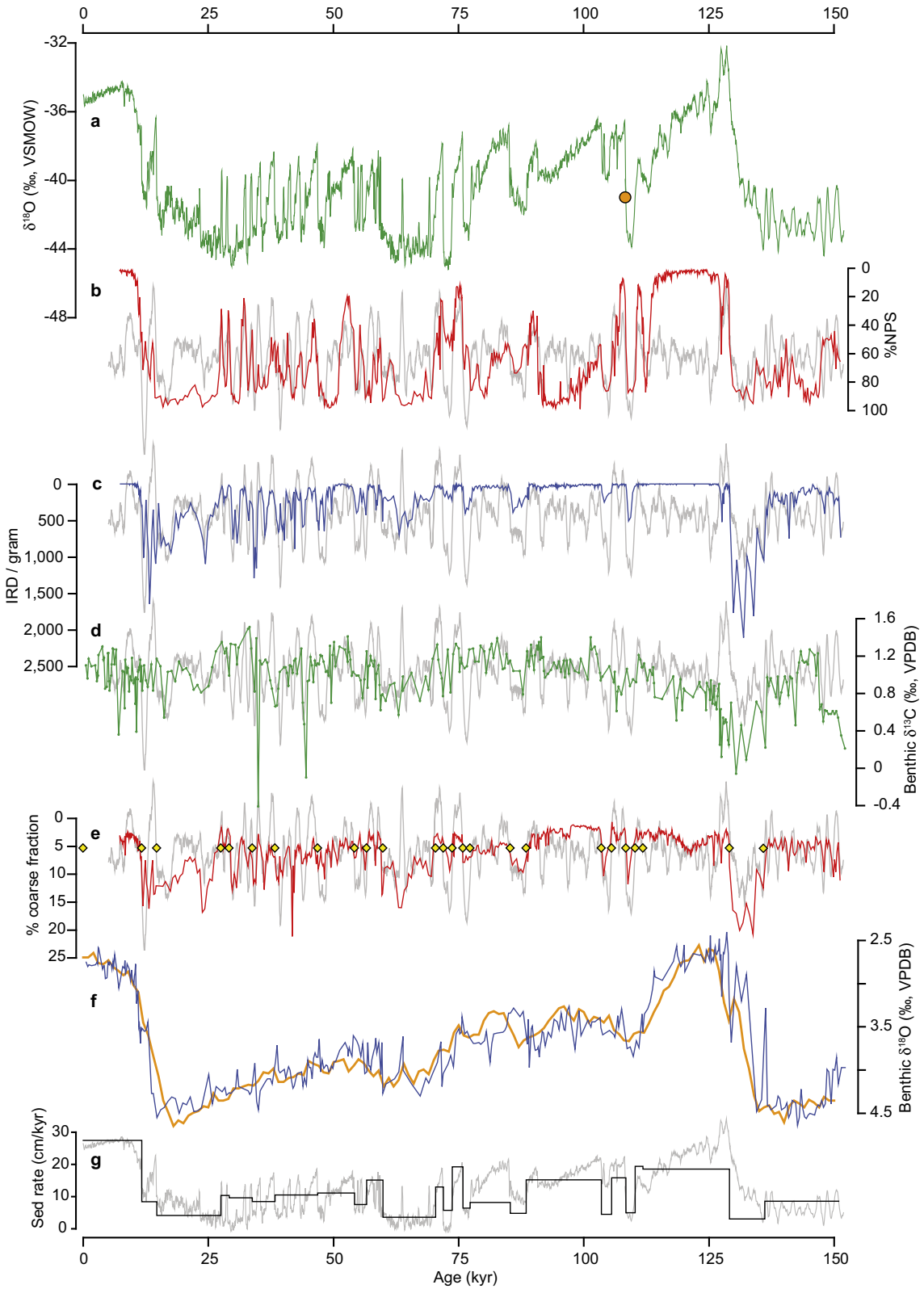

Extended Data Figure 4 | Age model development for ODP site 983 (0–150 kyr ago). **a**, Splice (at orange circle) of NGRIP $\delta^{18}O$[2] and a synthetic Greenland temperature record, GL_T_syn[48]. **b**, %NPS. **c**, IRD per gram. **d**, Benthic $\delta^{13}C$ (ref. 26). **e**, Per cent coarse fraction (yellow symbols are tuning points). **f**, Benthic $\delta^{18}O$ from ODP site 983 (ref. 26) (blue curve) with LR04 stack (shifted by −0.5‰; orange curve) for comparison. **g**, Sedimentation rates implied by new age model. All records (except LR04 stack) are on the GICC05 age model[53] back to 60 kyr ago and a modified version of the speleothem-tuned age model of ref. 48 (using the NALPS speleothems[54] between 60 kyr ago and 108 kyr ago) for older ages[52]. The grey curve in **b**–**e** is the millennial-scale component of GL_T_syn ($GL_T\_syn\_hi$)[48].

©2015 Macmillan Publishers Limited. All rights reserved

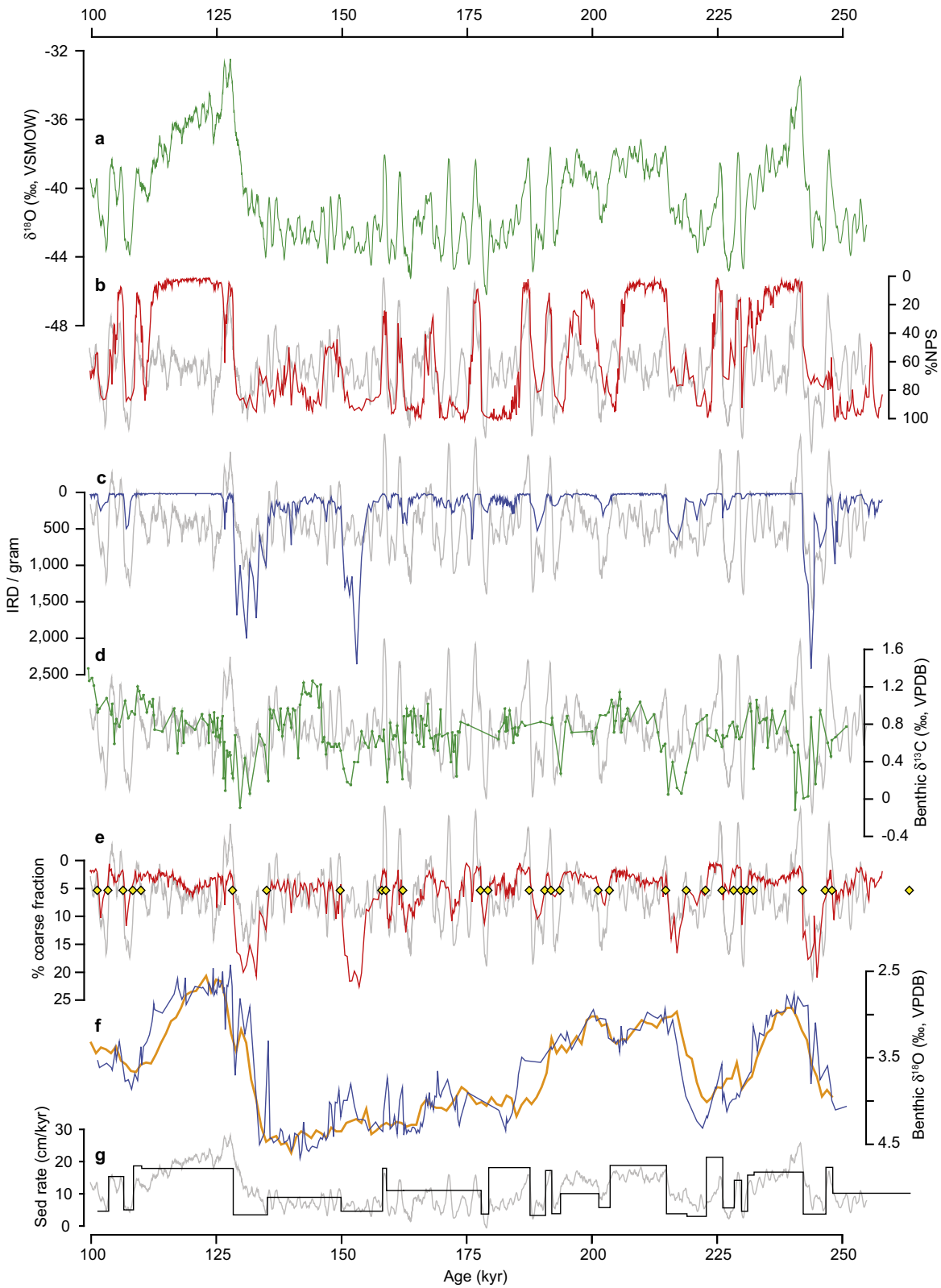

Extended Data Figure 5 | Age model development for ODP site 983 (100–250 kyr ago). **a**, Synthetic Greenland temperature record, GL_T_syn[48]. **b**, %NPS. **c**, IRD per gram. **d**, Benthic $\delta^{13}C$ (ref. 26). **e**, Per cent coarse fraction (yellow symbols are tuning points). **f**, Benthic $\delta^{18}O$ from ODP site 983 (ref. 26) (blue curve) with LR04 stack (shifted by −0.5‰; orange curve) for comparison. **g**, Sedimentation rates implied by new age model. All records (except the LR04 stack) are on the EDC3 age model[49]. The grey curve in **b**–**e** is the millennial-scale component of GL_T_syn ($GL_T\_syn\_hi$)[48].

©2015 Macmillan Publishers Limited. All rights reserved

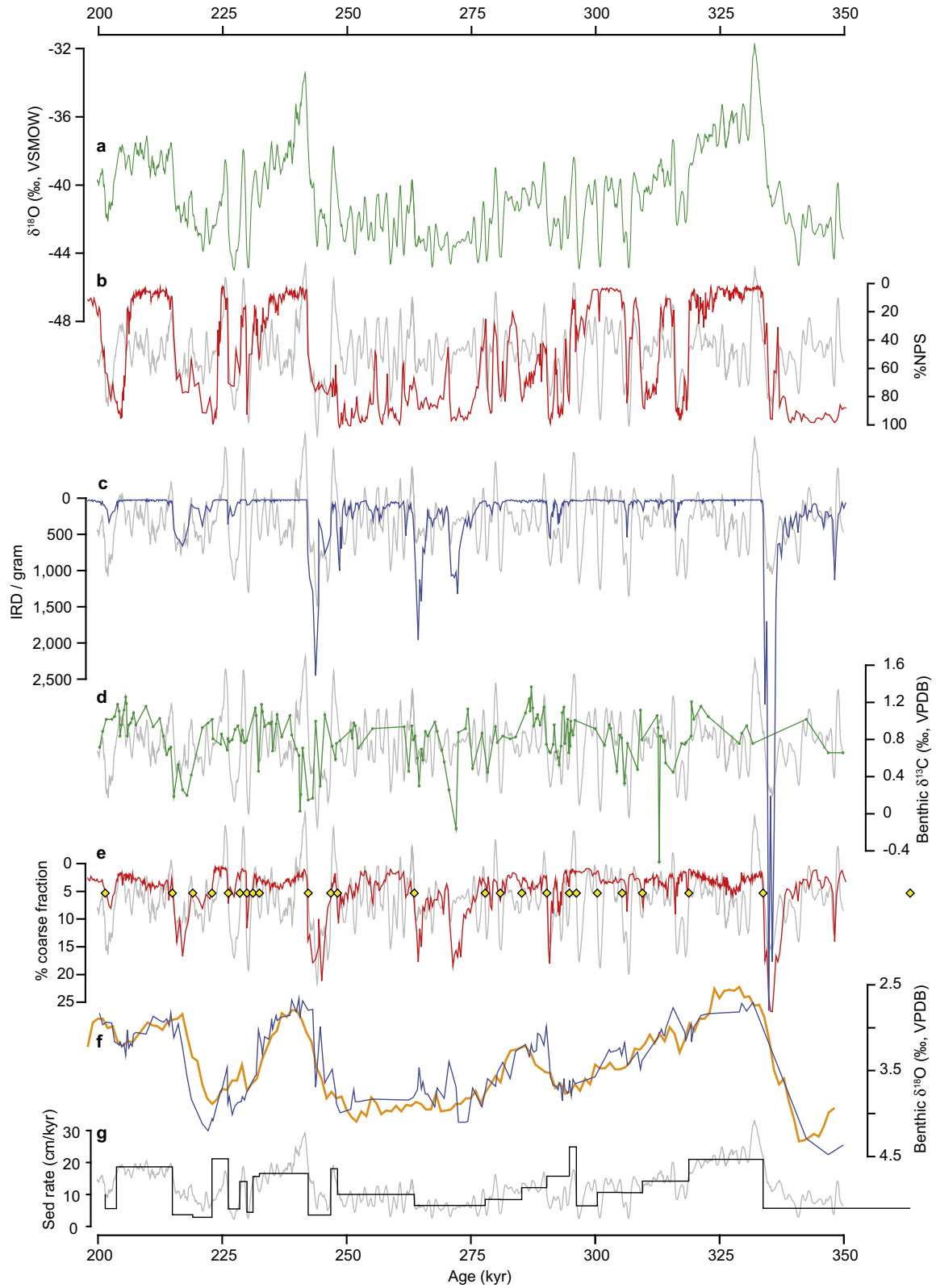

Extended Data Figure 6 | Age model development for ODP site 983 (200–350 kyr ago). **a**, Synthetic Greenland temperature record, GL_T_syn[48]. **b**, %NPS. **c**, IRD per gram. **d**, Benthic $\delta^{13}C$ (ref. 26).**e**, Per cent coarse fraction (yellow symbols are tuning points). **f**, Benthic $\delta^{18}O$ from 983[26] (blue curve) with LR04 stack (shifted by −0.5‰; orange curve) for comparison. **g**, Sedimentation rates implied by new age model. All records (except the LR04 stack) are on the EDC3 age model[49]. The grey curve in **b**–**e** is the millennial-scale component of GL_T_syn ($GL_T\_syn\_hi$)[48].

©2015 Macmillan Publishers Limited. All rights reserved

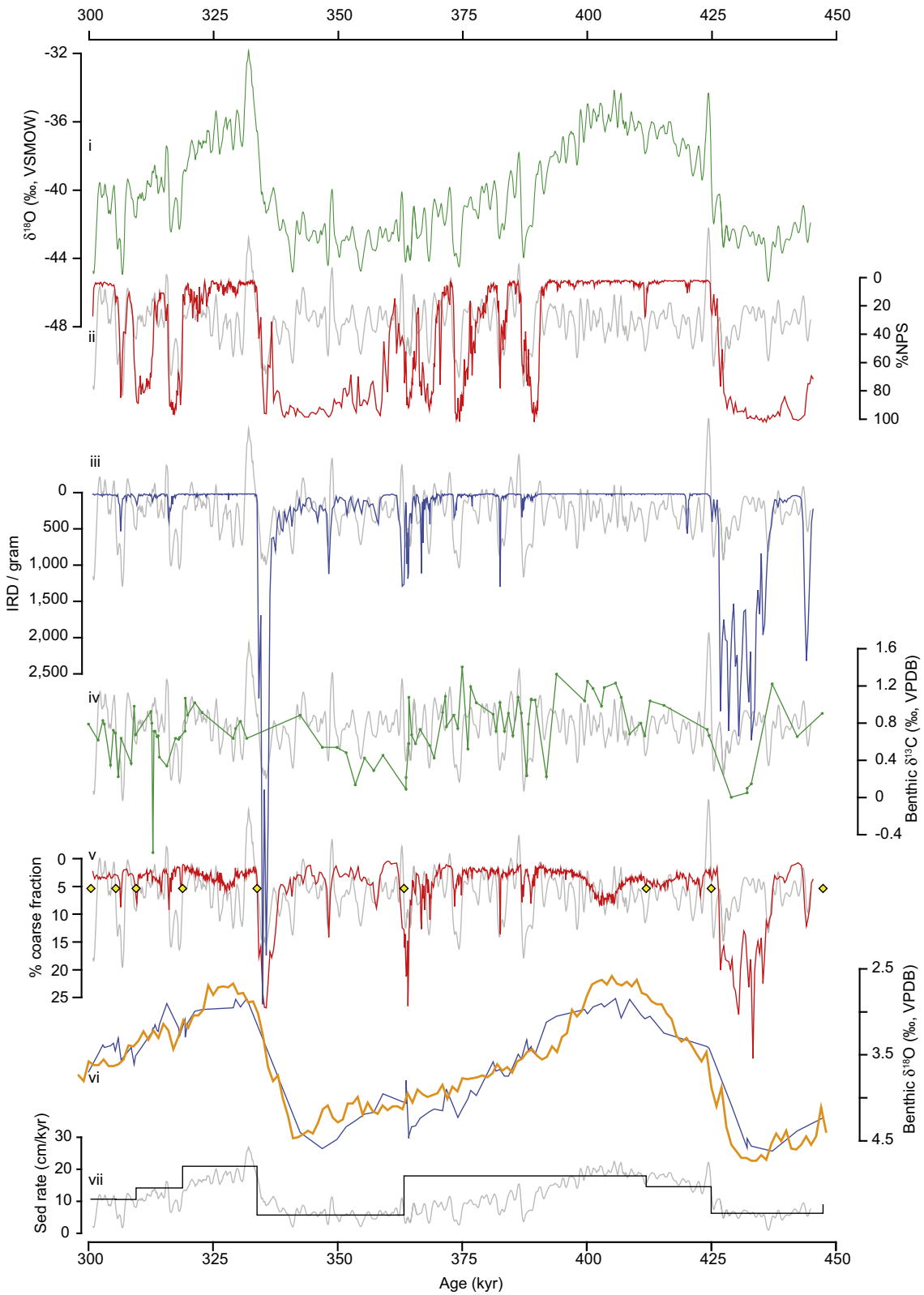

Extended Data Figure 7 | Age model development for ODP site 983 (300–450 kyr ago). **a**, Synthetic Greenland temperature record, GL_T_syn[48]. **b**, %NPS. **c**, IRD per gram. **d**, Benthic $\delta^{13}C$ (ref. 26). **e**, Per cent coarse fraction (yellow symbols are tuning points). **f**, Benthic $\delta^{18}O$ from ODP site 983 (ref. 26) (blue curve) with LR04 stack (shifted by −0.5‰; orange curve) for comparison. **g**, Sedimentation rates implied by new age model. All records (except the LR04 stack) are on the EDC3 age model[49]. The grey curve in **b**–**e** is the millennial-scale component of GL_T_syn ($GL_T\_syn\_hi$)[48].

©2015 Macmillan Publishers Limited. All rights reserved

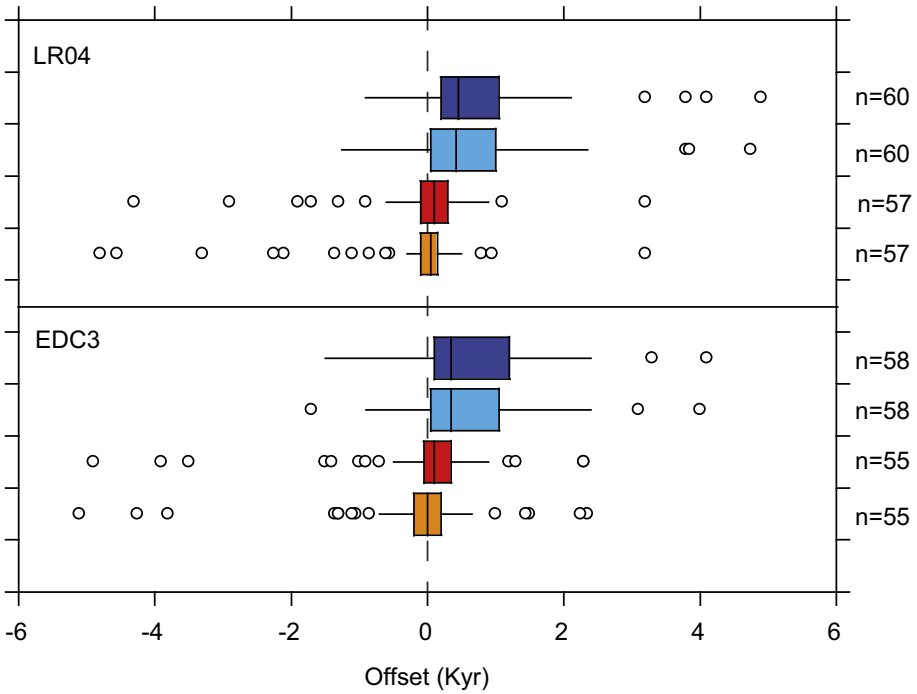

Extended Data Figure 8 | Cooling and warming offsets calculated using the revised age model Box and whisker plots show calculated offsets between temperature change (change in %NPS) and IRD at ODP site 983 using the LR04 age model (upper panel) and our revised EDC3 age model (lower panel). Boxes represent the interquartile range (IQR, 25%—75%) dissected by the median value. Whiskers are 1.5×IQR and extend to the last value included in this range. Positive values signify temperature change is earlier. Blue boxes represent cooling versus arrival of IRD; red/orange boxes represent warming versus IRD decrease. Dark blue/red boxes represent the start of a transition; light blue/orange boxes reflect the mid-point. *n* is the number of paired transitions detected.

©2015 Macmillan Publishers Limited. All rights reserved

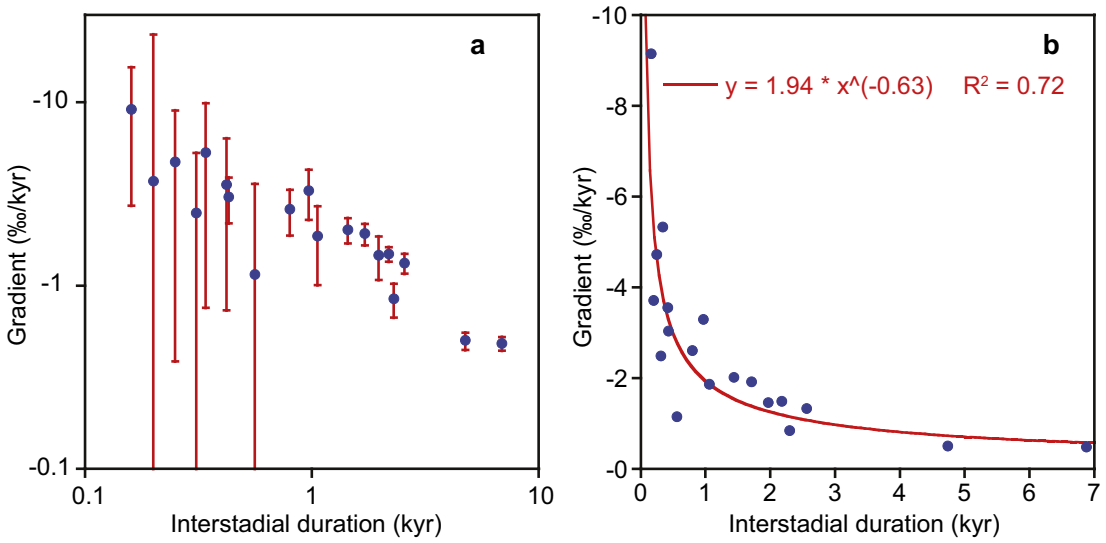

Extended Data Figure 9 | Rate of cooling (according $\delta^{18}O$) versus duration of an interstadial in the NGRIP ice core. a, Logarithmic scales (error bars represent the uncertainty in the calculated gradients). **b**, Linear scales. Interstadial durations were calculated using a thresholding approach on the first derivative of the smoothed $\delta^{18}O$ record[2] to identify their abrupt onsets and ends. 50 years were then subtracted from either end of each identified interval before calculating the gradients (using the raw, unsmoothed measurements) to avoid contamination from the sharp transitions. Shorter intervals have fewer data points and therefore greater scatter (leading to greater uncertainty in the calculated gradient). Two very short intervals (Dansgaard–Oeschger events 17 and 18) were omitted from the analysis. This analysis is an updated version of that made by Schulz[28] on the GISP2 ice core.

©2015 Macmillan Publishers Limited. All rights reserved